Egypt. J. Bot. **Vol. 61**, No.3, pp. 823-836 (2021)

Egyptian Journal of Botany
http://ejbo.journals.ekb.eg/

Pathological Changes in Sweet Basil (*Ocimum basilicum* L.) Caused by Mixed Infection of Tobacco Mosaic Virus and Phytoplasma

Yasmine Abuhadema, El-Sayed T. Abd El-Salam Sayed, Mahasen Ismail, Maha AlKhazindar[#]
Department of Botany and Microbiology, Faculty of Science, Cairo University, Cairo, Egypt.

OCIMUM basilicum L. (a medicinal plant known as sweet basil) was investigated and showed disease symptoms, including mosaic mottling, leaf distortion, blistering, witches' broom, and phyllody. The plants were found to be infected by both tobacco mosaic virus (TMV) and phytoplasma. Positive TMV was indicated by serological identification using direct antibody sandwich enzyme-linked immunosorbent assay (DAS-ELISA). Phytoplasma infection was identified molecularly using the phytoplasma P1/P7 primer pair and the nested primer, R16F2n/R16R2, which successfully generated a DNA band at ~1200 bp. The virus was successfully transmitted mechanically to *Nicotiana tabacum*, *Datura metal*, *Datura stramonium*, and *Phaseolus vulgaris*. Light and transmission electron microscopy showed pleomorphic phytoplasmas and rod-shaped particles (300 nm) of TMV, respectively. Histopathological and cytopathological studies revealed changes in the cell behavior of the infected leaves of sweet basil due to virus and phytoplasma infection. Hypoplasia and hyperplasia were observed in the mosaic areas of the mesophyll. Alterations in the vascular tissues and degeneration of the organelles were observed in ultrathin sections of the infected mesophyll. The presence of phytoplasma cells and crystalline bodies were indicative of the mixed infection. To our knowledge, this is the first report of a mixed infection of TMV and phytoplasmas in sweet basil.

Keywords: Cyto- histopathology, DAS-ELISA, Nested primer, Phytoplasma, Sweet basil, TMV.

Introduction

Medicinal plants play a vital role in human health and have been used to treat disease since ancient times. The *Ocimum* genus has a variety of species, including *Ocimum basilicum* L., *Ocimum sanctum* L., *Ocimum canum*, *Ocimum ammericanum*, and *Ocimum camphora* (Rubab et al., 2020). The *Ocimum* comprise around 100 herbs and shrubs that grow in the tropical and subtropical regions of the world. *Ocimum* originated from the Asian continent but is cultivated universally as a perennial, aromatic plant. Sweet basil is known for its pharmacological properties and can be used to treat cardiovascular diseases, diabetes, neurodegenerative disorders, menstrual cramps, cancer, and digestive disorders. It is also used as a culinary herb due to its pleasant flavor. In addition, sweet basil's antioxidant, antimicrobial, and larvicidal activities have been recorded (Purushothaman et al., 2018).

In Egypt, the cultivated areas of sweet basil are increasing, especially in the newly reclaimed lands, to meet the needs of local consumption and for export purposes. The Egyptian government has encouraged the expansion of medicinal and aromatic plant cultivation in Egypt (El-Saad & El-Saad, 2018). The local cultivated area in Egypt has now reached approximately 7,329 Feddan. During 2013, Egypt was ranked the fourth (41,664MT) sweet basil exporter in the world (El-Attar et al., 2019).

Many microorganisms can cause destructive

[#]Corresponding author email: malkhazi@aucegypt.edu
Received 29/4/ 2021; Accepted 05/09/ 2021
DOI: 10.21608/ejbo.2021.74591.1686
Edited by: Dr.: Mahmoud S.M. Mohamed, Faculty of Science, Cairo University, Giza 12613, Egypt.

disease in sweet basil, leading to a reduction in its quality and quantity. The available literature reveals that the most common viruses infecting sweet basil are alfalfa mosaic virus (Wintermantel et al., 2012; Bruni et al., 2016), broad bean wilt virus (Sanz et al., 2001), impatiens necrotic spot virus (Grausgruber-Gröger, 2012), tomato yellow leaf curl virus, tomato leaf curl Al Batinah virus, chili leaf curl virus (Ammara et al., 2015), pepino mosaic virus (Davino et al., 2009), and tomato spotted wilt virus (Holcomb et al., 1999). In addition, phytoplasmas are one of the most important pathogens that infect sweet basil, causing yield reduction and severe symptoms, such as chlorosis and distortion/streaking of the leaves (Arocha et al., 2006).

Any plant disease control relies on the accurate identification of the disease and its causative agent. Detection and diagnosis are therefore the most critical part of the management of plant viruses. The basis for detecting and identifying viruses are the biological, morphological, and intrinsic properties, which include serological and molecular techniques (Baranwal et al., 2021). Enzyme-linked immunosorbent assay (ELISA) is considered a sensitive and specific method for virus detection (Zahn et al., 2011).

The pathological impacts of viruses on plants have been documented in previous studies, where mesophyll and vascular cylinder abnormalities were found in infected plants (Hull, 2009; Otulak et al., 2015; Parrella et al., 2015; Alkhazindar et al., 2016). The Plant Virus Subcommittee of the International Committee on Taxonomy of Viruses (ICTV) listed inclusion bodies as one of the parameters for virus classification (Edwardson et al., 1986). To understand the relationship between the virus and the host plant it is necessary to study the anatomical changes in the host plant. One of the main changes caused by viral infection is growth abnormality (Esau, 1967). During multiplication of the causal agent in cells, certain pathological phenomena may occur, such as necrosis or hypoplasia (Schneider, 1973). Furthermore, viruses can disturb the internal organization of cells by altering their form, appearance, and arrangement (Stevens, 1983).

In this study, we report the presence of a mixed infection of TMV and phytoplasma in sweet basil using biological, serological, and molecular studies. The correlation between TMV and phytoplasma is reported through ELISA and nested-PCR in relation to climatic changes. Furthermore, we studied the changes in cell behavior and the anatomical and cytological alterations induced in leaves due to mixed infection.

Material and Methods

Sample collection

From 2017 to 2020, leaves of sweet basil that showed disease symptoms were collected from Cairo University campus, Giza. The aerial parts (stems and leaves) of the plants were collected and stored at −20°C. Normal seeds from the same species were grown in a greenhouse and the plants grown from these seeds were used as controls.

Mechanical transmission and single lesion transmission

Leaves of naturally infected sweet basil (1g) were ground using a sterilized mortar and pestle. Distilled water (2mL) was added, and the extract was filtered through cheesecloth. The inoculum was applied onto 600 mesh carborundum lightly dusted on 2-month-old healthy *Phaseolus vulgaris* plants. The inoculation was performed mechanically using the forefinger according to the method described by Hull (2009). The inoculated leaves were washed thoroughly with water and observed for any changes. The same experiment was repeated using healthy sweet basil plants as controls.

After 8 days of infection, a single lesion was cut from the infected *Phaseolus vulgaris* leaf and the extract was reinoculated on healthy sweet basil plants. The plants were washed and then placed in a controlled greenhouse and monitored for appearance of symptoms.

Host range

Eight different host plant species were tested as virus hosts: *Capsicum annuum*, *Datura metel*, *Datura Stramonium*, *Nicotiana tabacum*, *Phaseolus vulgaris*, *Petunia* sp. *Solanum lycopersicum*, and *Vicia faba.* The host plants were mechanically inoculated with sap extracted from a single lesion of the infected leaves. All plant species were grown from healthy seeds. All experiments were carried out in a greenhouse at 20–25°C.

Direct antibody sandwich enzyme-linked immunosorbent assay (DAS-ELISA)

DAS-ELISA was used against TMV according to the method described by Clark & Adams (1977),

with some modifications. Specific immunoglobulin G (IgG) for TMV was supplied by DSMZ (Braunschweig, Lower Saxony, Germany) and diluted (1:1000) using coating buffer (pH 9.6), as prescribed by the provided manual. Polyethylene microtiter plates were coated with IgG (200µL/well) and incubated overnight at 4°C. Wells were washed three times with PBS-Tween buffer (pH 7.4). Healthy and infected sweet basil leaves (0.3g each) were macerated in 1 ml of extraction buffer (pH 7.4) using a mortar and pestle, followed by centrifugation at 3000× *g* for 1min. The supernatant (200µL) was added to the wells and incubated at 4°C overnight. Wells were rewashed three times with PBS-Tween, and 200µL of IgG-AP conjugate diluted in conjugate buffer (pH 7) was pipetted into each well. Plates were then incubated at 4°C overnight. Plates were washed three times with PBS-Tween followed by the addition of 200µL/well of freshly prepared substrate (para-nitrophenyl-phosphate). The plates were incubated at 37°C for 45min. The absorbance was measured at 405 nm using an ELISA reader (Das, Italy). The results were considered positive when the readings were two times the readings of the control. DAS-ELISA was repeated monthly from July 2018 until June 2019.

DNA extraction and nested PCR assay

Total nucleic acid was extracted from leaf midribs and petioles (100mg) using an EZ-10 Spin Column Plant Genomic DNA Miniprep Kit (Bio Basic Inc., Canada). The purity and concentration of nucleic acid was determined using a Q3000 UV spectrophotometer (Quawell, USA). PCR was carried out with 25µL PCR master mix (Genedirex), 1µL DNA, 1µL of each primer (P1/P7;10 pmol), and 22µL distilled sterile water. The amplification cycles comprised a 3-min denaturation step at 95°C, followed by 35 cycles at 94°C for 1min, 50°C for 2min, and 72°C for 3min, and a final extension step at 72°C for 10min. The PCR product was diluted (1:20) and used as a template for nested PCR using the R16F2n/R16R2 primer pair targeting the 16s rRNA gene under the same conditions as those described above (Bertaccini et al., 2019a).

Gel electrophoresis

PCR product (5µL) was electrophoresed in 1% agarose gel using 1× Tris-borate-EDTA buffer, stained with ethidium bromide (0.5µg/mL), and photographed using gel documentation (MicroDoc, Cleaver Scientific, UK). The fragments length was estimated by comparing them to O'RangeRuler 100+500 bp DNA Ladder, ready-to-use (Thermo Fisher Scientific, USA).

Virus purification

Infected sweet basil was used as a source for virus purification, according to the method described by Chapman (1998). Twenty grams of infected leaves were homogenized in 4mL extraction buffer (1% (v/v) 2-mercaptoethanol in 0.5M phosphate buffer just before use) using a mortar and pestle. The homogenate was filtered through two layers of cloth. Butanol (0.8mL/10mL of filtrate) was added dropwise to the filtrate while swirling the tube contents. The tubes were incubated at room temperature for 15 min and mixed every few minutes. The tubes were centrifuged at 10,000× *g* for 30min at 12°C. Polyethylene glycol (PEG) solution (20%) was added and mixed with 0.4mL/10mL of supernatant, followed by incubation on ice for 15min. The mixture was centrifuged at 10,000× *g* for 15min at 4°C. The supernatant was discarded, and the pellet was dissolved in 8mL of 10mM phosphate buffer. This was followed by centrifugation at 10,000× *g* for 15min at 4°C. The supernatant was transferred to a fresh tube and 1.7mL of 5M NaCl and 2.24mL of 20% PEG were added. The solution was mixed and then incubated on ice for 15min. Centrifugation was then performed at 10,000× *g* for 15min at 4°C, and the supernatant was discarded. The pellet was dissolved in 2mL of 10mM phosphate buffer. The solution was divided into two 1.5mL centrifuge tubes for centrifugation at 13,000× *g* for 30s, then the supernatant was pipetted into a fresh microcentrifuge tube.

Determination of virus purity

The purity of virus particles in the supernatant was evaluated using a Q3000 UV spectrophotometer (Quawell, USA) to measure the UV absorption spectra and to determine the ratio of A260/A280.

Electron microscopy

A drop of purified virus was loaded on a carbon-coated grid, stained with 2% phosphotungstic acid (pH 7.0), and allowed to air dry. The grid was then examined under transmission electron microscopy (TEM) (JEOL; JEM-1400 TE, Japan) at the desired magnification. Images were captured using a charge-coupled device (CCD) camera (model AMT). This work was conducted at the TEM laboratory of the Faculty of Agriculture Research Park (FARP), Cairo University.

Anatomical studies using light microscopy

To test for the presence of phytoplasma, sections of healthy and infected main veins, shoots, and petioles of sweet basil were cut using a microtome and placed in distilled water. The sections were incubated in Dienes' stain for 10 min at room temperature, then washed in distilled water, mounted in water, and observed under light microscopy (Musetti, 2013).

Histopathological and cytopathological studies

Naturally infected leaves that were showing symptoms were chosen for sectioning for the histopathological and cytopathological studies. Phenotypically normal leaves grown in the greenhouse were used as controls. The method described by Alkhazindar & Sayed (2016) with some modifications was used as the technique for the preparation of permanent slides for microtome sections. Leaf sections were fixed in Nawaschin type (Craf) II (1% chromic acid, 10% acetic acid, and 10% formaldehyde), dehydrated in different concentrations of ethyl alcohol and tertiary butyl alcohol, embedded in paraffin wax, and sectioned. The sections were stained with erythrosine. Stained sections were examined under light microscopy.

The same areas and control leaves that were chosen for histopathology were used for the cytopathological studies. Ultrathin sections were fixed in 1% glutaraldehyde and osmium tetroxide, dehydrated in alcohol, and embedded in epoxy resin. Microtome sections were prepared in approximately 500–1000-pm thicknesses with a Leica Ultra Cut UCT ultramicrotome. Sections were stained with toluidine blue (IX), and were examined by camera (Leica ICC50 HD). Ultrathin sections were prepared at approximately 75–90-µm thicknesses and stained with uranyl acetate and lead citrate, then examined under transmission electron microscopy (JEOL; JEM-1400 TEM) at the desired magnification. Images were captured by charge-coupled device (CCD) camera (model AMT), and an optronics camera with a 1632× 1632-pixel format as the side-mount configuration. This camera uses a 1394-fire wire acquisition board. This work was conducted in the TEM laboratory of FARP, Cairo University.

Results

Disease symptoms

Sweet basil samples were collected from Cairo University campus, Giza, between 2017 and 2020. The symptoms varied during the seasons and included mosaic mottling, leaf distortion, blistering, downward leaf curling, and crinkling during January and February (winter), as shown in Fig. 1. However, the symptoms included witches' broom, excessive branching of axillary shoots, black streaks on the stem, and phyllody during March and April (spring), as shown in Fig. 2.

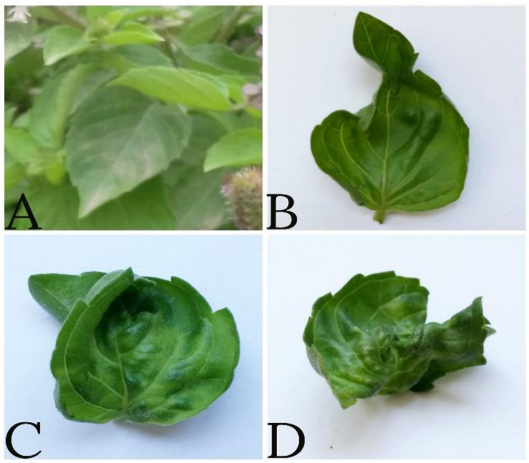

Fig. 1. Naturally infected sweet basil plants during winter (10°C–20°C) showing viral infection [(A) Control plant, (B) Blistering and leaf distortion, (C) Mosaic mottling (light and dark green areas), blistering and leaf distortion, (D) Mosaic mottling, crinkling, and leaf distortion]

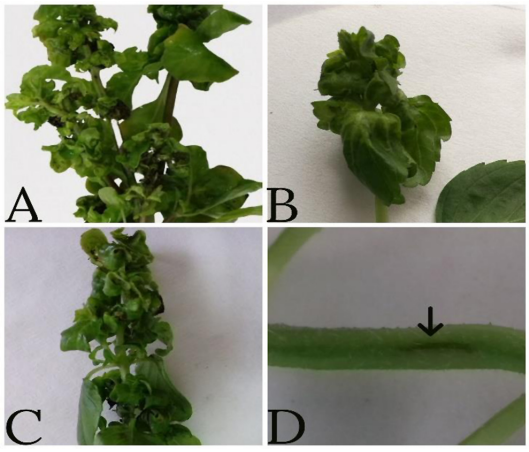

Fig. 2. Naturally infected sweet basil plants during spring (25°C–30°C) showing phytoplasma infection [(A) Shoot proliferation, (B) Witches' broom, (C) Phyllody, (D) Black streaks on the stem (arrowhead)]

Mechanical transmission and single-lesion transmission

The sap from sweet basil infected leaves

was mechanically inoculated onto *D. metel* plants. A single chlorotic local lesion was cut and reinoculated to normal (healthy) sweet basil plants. The same viral symptoms appeared on the inoculated plants after 3 weeks.

Host range

The virus was mechanically transmitted to *Nicotiana tabacum*, *Datura metel*, *and Datura Stramonium*, and these plants formed chlorotic local lesions after approximately 7 days. *Phaseolus vulgaris* showed necrotic local lesions 3 days after inoculation (Fig. 3). However, *Capsicum annuum*, *Petunia* sp. *Solanum lycopersicum*, and *Vicia faba* did not show any symptoms.

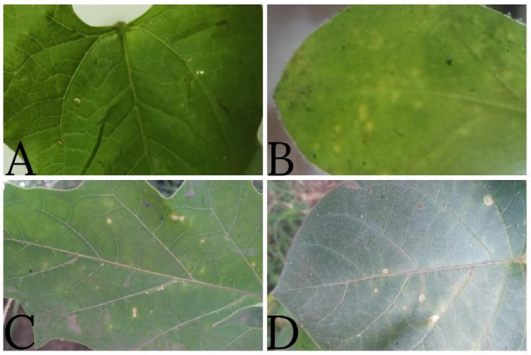

Fig. 3. Symptoms produced on different hosts using mechanical inoculation from sweet basil after single-lesion transmission [(A) Necrotic lesions on *Phaseolus vulgaris*, chlorotic local lesion on (B) ***Nicotiana tabacum,*** (C) ***Datura Stramonium,*** **and** (D) ***Datura metel*****]**

DAS-ELISA

DAS-ELISA using IgG against TMV detected the presence of the virus in infected sweet basil. The TMV concentration was recorded monthly from July 2018 until June 2019. Reactions were considered positive when the readings were two times higher than the control. The generated data revealed a significant correlation between climatic changes and TMV concentration. High concentrations of TMV were detected during July, August, and September: 0.541, 0.794, and 0.239, respectively. However, the TMV concentration decreased during the rest of the year (Table 1).

Nucleic acid extraction, PCR, and nested PCR

Total DNA was extracted from sweet basil. The purity ratio of the produced DNA was 1.9, with a concentration of 996ng/µL. PCR using the universal primer pair P1/P7 showed a faint product. However, DNA was amplified when proceeding with nested PCR using specific primers of phytoplasma (R16F2n/R16R2). A specific band at ~1200 bp was obtained (Fig. 4).

Virus purification and electron microscopy

The concentration of the purified virus was 116 ng/µl, with a purity ratio of 1.32. The purified virus was examined under transmission electron microscopy. Rod-shaped virus particles measuring ~300nm in length and ~26nm in width were observed (Fig. 5).

Anatomical studies using light microscopy

Sections of the infected stems of sweet basil showing necrotic streaks and stained using Dienes' stain showed phytoplasma pleomorphic bodies. The phytoplasma cells were localized in the phloem tissues and were stained blue (Fig. 6).

TABLE 1. Absorbance values at 405nm obtained for the determination of TMV using DAS-ELISA during different seasons

Season	Month	Virus concentration expressed as Absorbance at 405nm		Results
		Infected	Control	
Summer (35°C–42°C)	July 2018	**0.541**	**0.225**	**Positive**
	August 2018	**0.794**	**0.418**	**Positive**
Fall (25°C–30°C)	Septemper2018	**0.239**	**0.112**	**Positive**
	October 2018	0.195	0.195	Negative
	November 2018	0.239	0.136	Negative
Winter (10°C–20°C)	December 2018	0.21	0.223	Negative
	January 2019	0.246	0.24	Negative
	February 2019	0.325	0.24	Negative
Spring (25°C–30°C)	March 2019	0.235	0.152	Negative
	April 2019	0.2	0.193	Negative
	May 2019	0.112	0.144	Negative
Summer (35°C–42°C)	June 2019	0.14	0.125	Negative

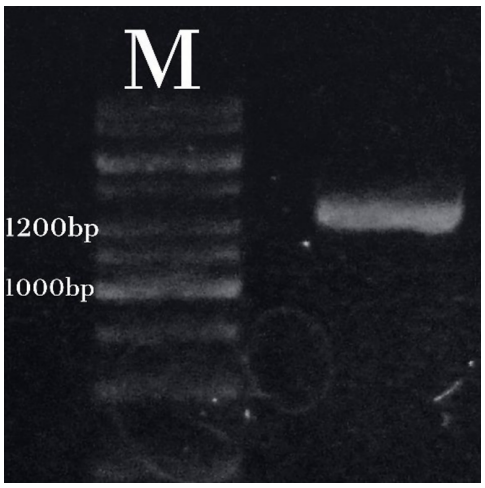

Fig. 4. 1% agarose gel electrophoresis showing nested PCR of phytoplasma in sweet basil using the specific primer pair, R16F2n/R16R2 [A specific band appeared at ~1200bp. M, marker O'RangeRuler 100+500bp DNA Ladder, ready-to-use]

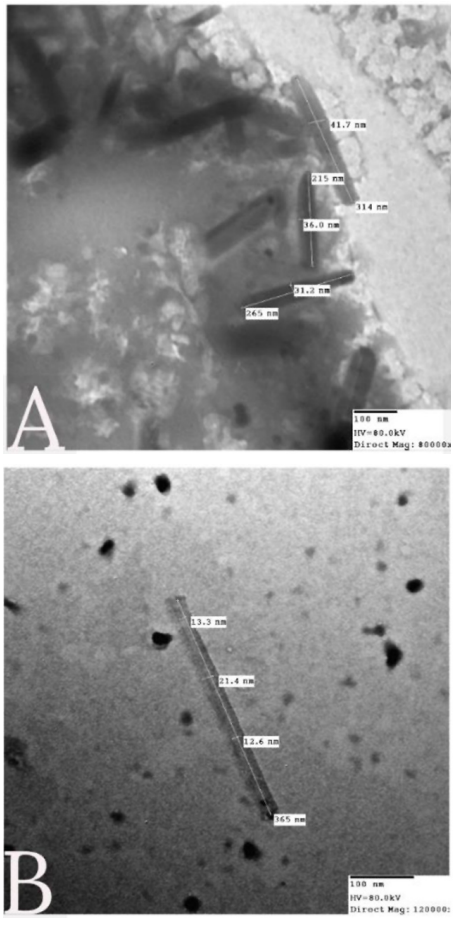

Fig. 5. Electron micrograph showing TMV particles in purified preparation negatively stained with 2% phosphotungstic acid [(A) A group of virus particles at ×80,000 magnification. (B) A single viral particle at ×120,000 magnification]

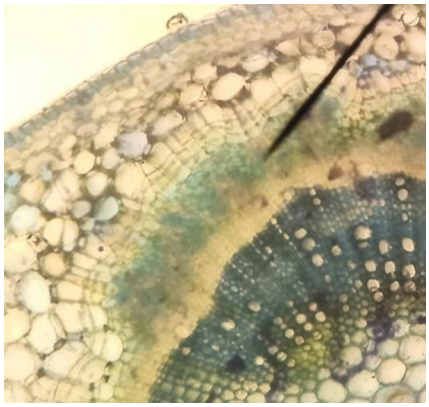

Fig. 6. Cross-section of an infected sweet basil stem stained with Dienes' stain showing pleomorphic bodies of phytoplasma

Histopathological studies

Cross-sections of healthy sweet basil leaves passing through the midrib showed normal anatomical features. The mesophyll consisted of palisade and spongy tissues filled with chloroplasts. The vascular tissue consisted of arranged xylem vessels and phloem above the protoxylem (Fig. 7).

Fig. 7. Section through the midvein portion of a simple foliage leaf on the main stem of a healthy sweet basil plant (Nassar et al., 2014)

Cross-sections passing through infected leaves with mosaic mottling, blistering, and leaf distortion showed a lignified and distorted lower epidermis accompanied by malformation. The blade formed a convex and concave curvature with asymmetric thickness of the mesophyll (Fig. 8). Sections passing through the light green areas showed thinner lamina compared to sections passing through the darker green sections. The mesophyll was undifferentiated into palisade and spongy tissues, indicating hypoplasia. The cells were compact, with few intercellular spaces. Few chloroplasts were observed in the yellow sections (Fig. 9).

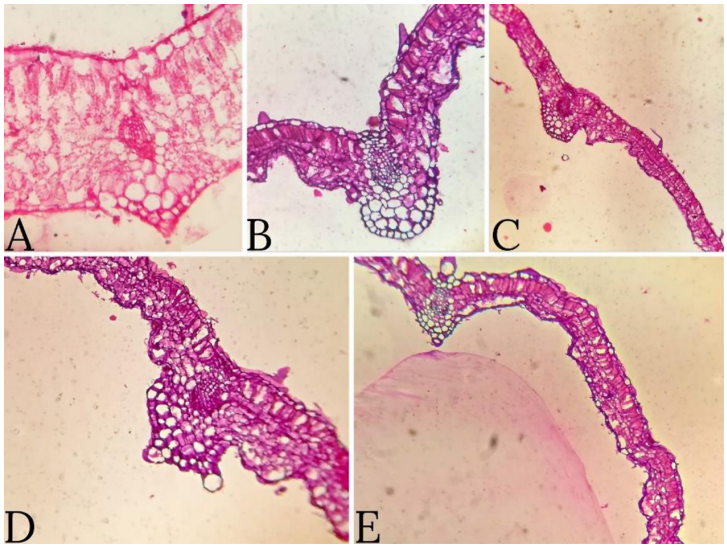

Fig. 8. Cross-section of infected midrib from sweet basil leaves [(A) Pointed and lignified lower epidermis, mosaic mottling and blistering. (B, C, D) Uneven mesophyll thickness, malformation, and abnormal midrib, (E) Downward bending of the leaf blade]

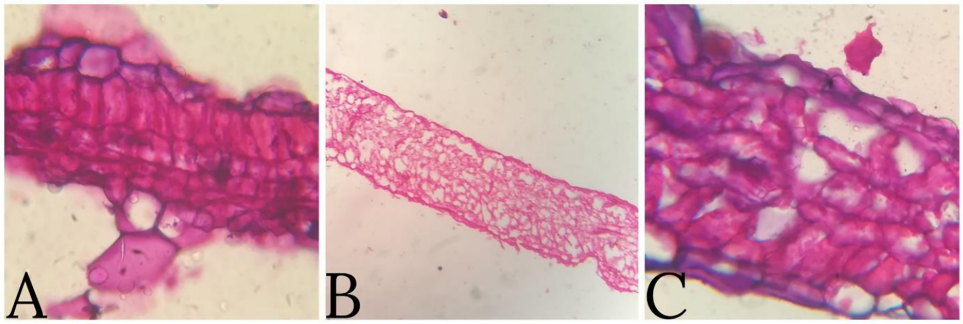

Fig. 9. Cross-section of infected sweet basil leaves passing through yellow banding showing [(A) Compact palisade and spongy tissue with almost no intercellular spaces, (B) Undifferentiated mesophyll tissue, (C) Enlarged section of undifferentiated mesophyll tissue]

Sections passing through the green vein banding showed hyperplasia, in which the number of mesophyll cells are increased, causing an increase in the thickness of the lamina (Fig. 10). The vascular tissue appeared small in size, with a reduced number of cells (Fig. 11), while excessive formation of vascular bundles appeared in other leaves (Fig. 12).

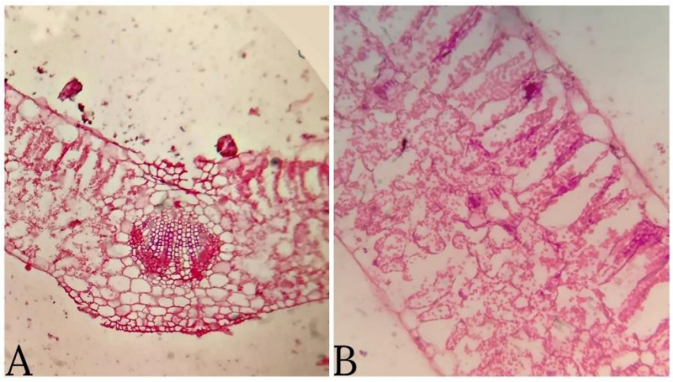

Fig. 10. Cross-section of infected sweet basil leaves passing through band of green vein [(A) Thick lamina with increased numbers of cells (hyperplasia), (B) Enlarged lamina with increased numbers of spongy tissues]

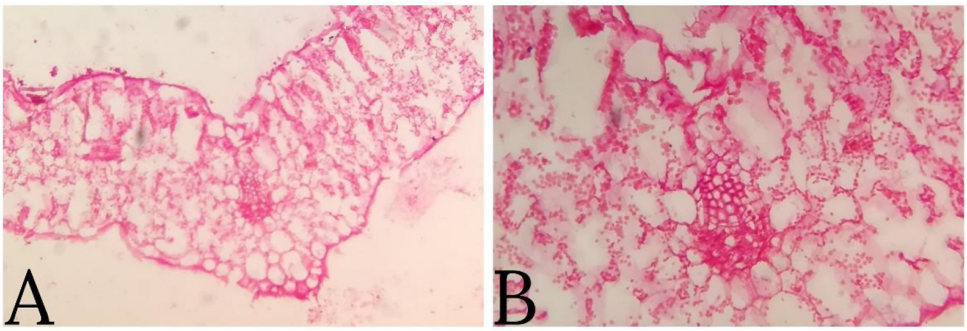

Fig. 11 . Cross-section of the midrib of infected sweet basil leaf showing a reduction in vascular bundles (A), (B) Magnified part showing a reduced number of xylem and phloem vessels

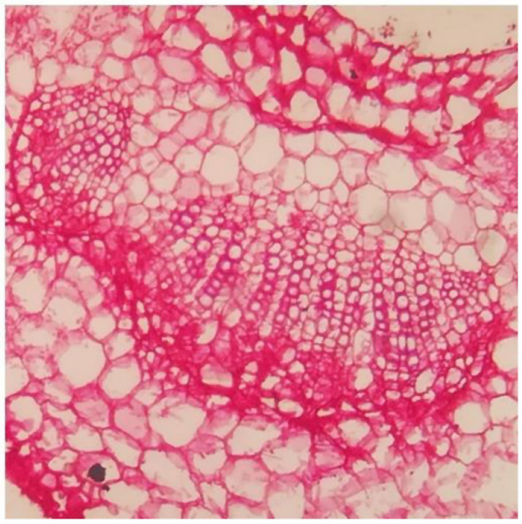

Fig. 12 . Cross-section of the midrib of infected sweet basil leaf showing the formation of excess vascular bundles

Cytopathological studies

Transmission electron micrography of the mesophyll cells of infected sweet basil revealed cytological alteration. The cell organelles appeared deformed and degenerated compared to the control, accompanied with an increase in the cell wall thickness (Fig. 13). Groups of paracrystalline, fibrous, spindle-shaped inclusions appeared in the cytoplasm. Typical hexagonal crystals were also detected in some sections (Fig. 14). A pleomorphic, wall-less structure appeared, indicating the presence of phytoplasma (Fig. 15).

Discussion

Sweet basil is an important medical herb. Several viral diseases reduce its yield and productivity. In our study, sweet basil was observed to show severe symptoms in the field during winter and spring, and the symptoms varied according to the weather conditions. During winter, viral symptoms, were more pronounced, while during spring, typical phytoplasma symptoms, were observed. All symptoms disappeared during the summer. Our results correlate with those of Fraser & Loughlin (1982), who studied the temperature dependence on TMV distribution in plants. Li et al. (2009) attributed symptom expression during winter to virus replication and movement, thus resulting in severe symptom formation. Conversely, during the summer season (high temperatures), virus replication and movement is prohibited, resulting in no foliar symptoms of infection. In fall and spring, symptoms are mild because the virus is in its early phase of increase and the host defense mechanism is high (Honjo et al., 2020).

In our study, sweet basil showed Witches' broom or proliferation and phyllody. These conditions are caused by changes in the normal growth patterns of the plant due to phytoplasma infection (Ermacora & Osler, 2019). Witches' broom occurs due to a loss of apical dominance, causing the proliferation of axillary shoots, which can be associated with decreased internode length. Therefore, the plant produces leaf-like structures instead of flowers. The remaining flowers are sterile and do not germinate (Ermacora & Osler, 2019). These symptoms appear during spring, when new phloem is formed (Marcone, 2009).

Our study showed that TMV can be mechanically transmitted as reported before by (Heinlein, 2002; Jung et al., 2002). Chlorotic local lesions appeared on *Datura metel*, where a single lesion was successfully back-inoculated on sweet basil and the same viral symptoms naturally appeared.

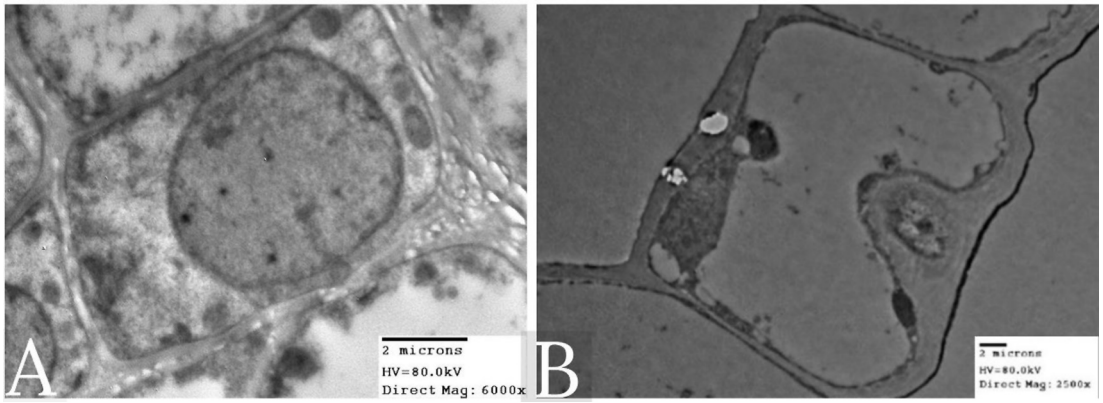

Fig. 13 . Electron micrographs of ultrathin sections of infected/control sweet basil leaves [(A) Control cell, (B) Infected cell showing abnormal cell wall thickness and abnormal protrusion to inside the cell]

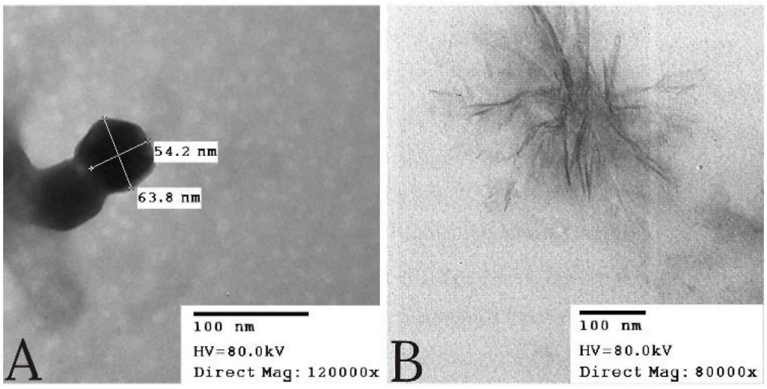

Fig. 14. Electron micrograph of ultrathin sections of infected sweet basil leaves showing (A) Typical hexagonal crystals in the cytoplasm, and (B) Groups of paracrystalline, fibrous inclusions

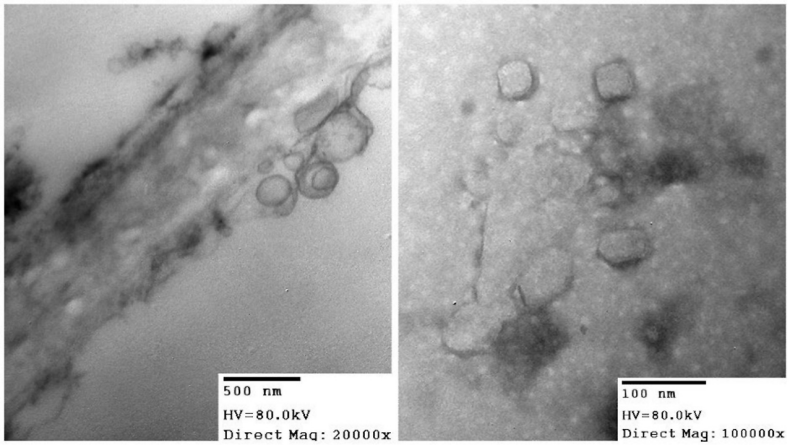

Fig. 15 . Electron micrograph of ultrathin sections of infected sweet basil leaves showing the pleomorphic, wall-less structure of the phytoplasma

In our study, we tested the mechanical transmission of TMV on some host plants. Local necrotic lesions appeared on *Phaseolus vulgaris*. This is in accordance with the study by Wu & Rappaport (1961), who reported the appearance of dark brown lesions on *P. vulgaris*, a differential host for TMV. In our study, *N. tabacum* was systemically infected; however, *Capsicum annuum*, *Petunia* sp. *Solanum lycopersicum*, and *Vicia faba* did not show any symptoms of infection. These results correlate with those of Sastry et al. (2019), who showed that these plants are not within the host range of TMV.

In our study, serological and molecular studies were used to identify the causative pathogens. DAS-ELISA using specific IgG identified the infection by TMV, while PCR and nested PCR confirmed that the sweet basil was also infected by phytoplasma. TMV concentration was highly affected by climatic changes and the presence of phytoplasma. The TMV titer was high during the summer (July, August, and September) and was decreased during the rest of the year. Furthermore, the presence of phytoplasma was detected when the phytoplasma symptoms were severe during the spring. Phytoplasma was tested using nested PCR, which generated a DNA band at the expected size (~1200bp). Our results are in accordance with those of Bertaccini et al. (2019a, b), who reported the presence of phytoplasma using specific primers targeting the 16s rRNA gene of the same size.

Our results confirm the co-existence of two pathogens (TMV and phytoplasma) in sweet basil plants. The co-existence of phytoplasma and viruses is well documented in many plants (Arocha et al., 2009). In pepper plants, a mixed infection of phytoplasma with two begomoviruses was previously reported in Mexico (Lebsky et al., 2011).

In our study, electron microscopy of partially purified virus revealed the presence of rod-shaped particles with an average length of 300nm and a width of 26nm, resembling that reported by Carr (2018), who described the shape and size of TMV particles. Phytoplasma cells were visualized using light microscopy. Pleomorphic bodies appeared in the phloem in the form of irregular patches of intensely dark blue stained cells. Our results match those described by Musetti (2013) and Ong et al. (2021), who described the shape and size of phytoplasma.

We studied the histopathological alterations accompanying the mixed infection. The anatomical features of the control sections were as described by Nassar et al. (2014). The sections of the infected leaves with mosaic symptoms showed hypoplasia in the yellow mottled areas, where the tissues were shorter and compactly arranged compared to healthy tissues, with fewer or no intercellular spaces. The lamina was thinner than in the dark green areas, and the mesophyll cells were less differentiated. The blade formed a convex and concave curvature, with asymmetric thickness of the mesophyll. The downward bending of the leaf blade was attributed to changes in meristematic activity, which is responsible for the development of the specific leaf form. In leaves that are still growing at the time of infection, a reduction in the activity of marginal meristems prevents the normal expansion of the lamina, which may cause reduction in the apical growth of the leaf (Esau, 1967).

In our study, sections of leaves showing viral symptoms passing through the midrib showed reduced vascular tissues with a low number of phloem cells and xylem vessels, while sections of leaves with viral and phytoplasma symptoms showed excessive vascular tissues, suggesting that these areas are particularly prone to hyperplasia. Similarly, in cacao swollen shoot virus (CSSV) infection, abnormal amounts of xylem tissue are produced, but cells are structurally normal (Hull, 2009). Moreover, infected tobacco plants showed hypertrophy of phloem parenchyma cells adjacent to sieve tubes, followed by the differentiation of many daughter cells into sieve tubes, causing an increase in their number (Schneider, 1973). The excessive formation of phloem tissue, resulting in swollen veins, may also occur due to phytoplasma infection (Lee et al., 2000).

Viral infection is responsible for many alterations in the infected tissues. Certain characteristic pathologic phenomena may happen in cells when multiplication of the causal agent occurs. These phenomena include increases in the thickness of the cytoplasm, deterioration of organelles and membranes, and the abnormal appearance of structures, such as inclusion bodies or virions aggregated into paracrystalline bodies (Schneider, 1973).

We observed abnormal thickness of the cell wall, abnormal protrusion to inside the cell, and the abnormal appearance of certain inclusion bodies. Cytoplasmic crystalline inclusions are a distinguishing feature of tobamovirus infections (Edwardson et al., 1978). Inclusion bodies have been defined as "intracellular structures produced *de novo* as a result of viral infection". These structures may contain virus particles, virus-related materials, or ordinary cell constituents in a normal or degenerate condition, either singly or, more often, in various proportions (Martelli & Russo, 1977). Inclusion bodies differ in form from amorphous structures to well-defined crystalline

structures; some of them are large enough to be seen under light microscopy, while others can only be detected under electron microscopy (Stevens, 1983). The paracrystalline, fibrous, spindle-shaped inclusions are composed of linear aggregates of virus particles united end-to-end (Esau, 1967). Furthermore, some light microscope studies have indicated that virus crystals develop in the X-bodies; in fact, the X-body may be completely converted into crystalline material. Consequently, at least some of the protein of the X-body is used to form the capsids of the virus particles, and the rest remains as noninfectious virus protein (Esau, 1967).

Members of the tobamovirus family cause virus particles to accumulate in crystalline arrays that appear as hexagonal or rounded plates (Martelli et al., 1977). We found that, in systemically infected plants and in localized lesions, bundles of paracrystalline needles occurred in vacuoles and typical hexagonal crystals occurred in the cytoplasm. The needles gave a protein reaction and were similar to the TMV inclusions previously described by other researchers (Esau, 1967).

Conclusion

To the best of our knowledge, TMV has not been reported as a pathogen that infects sweet basil. Therefore, this study reports sweet basil as a new host of TMV. Moreover, our findings are indicative for the co-existence of TMV and phytoplasma. The presence of both pathogens was correlated with climatic changes. This was studied by DAS_ELISA and nested-PCR. Histological and cytopathological alterations caused by mixed infection accompanied changes in phenotypic symptoms.

Although this study provides evidence for the co-existence of phytoplasma and TMV, additional studies are recommended to understand the synergism between the virus and phytoplasma in mixed infection under natural conditions, the mechanisms by which these pathogens are transmitted together to the same plant host, and other factors, such as their single and combined effect on sweet basil, their extent throughout the country, and the factors determining their coexistence, in addition to any epidemiological implications and impacts that may occur from geographic location and/or climate conditions. Disease severity and yield loss may be increased by mixed infection as compared to single infection. Therefore, the synergistic interactions between viruses and phytoplasmas should explored in further studies.

Conflict of interests: The authors declare no conflict of interest.

Authors contribution: All authors have contributed equally in conceptualization, methodology design, the laboratory work, interpretation of the results and preparing the manuscript.

Ethical approval: Not applicable

References

Alkhazindar, M., Sayed, E.T.A. (2016) Histo-Cytopathological changes in F*icus carica* L. infected with tomato spotted wilt Tospovirus. *Minia Science Bulletin*, **27**, 1-18.

Ammara, U.E., Al-Ansari, M., Al-Shihi, A., Amin, I., Mansoor, S., Al-Maskari, A.Y., Al-Sadi, A.M. (2015) Association of three begomoviruses and a betasatellite with leaf curl disease of basil in Oman. *Canadian Journal of Plant Pathology*, **37**, 506-513.

Arocha, Y., Piñol, B., Picornell, B., Almeida, R., Jones, P., Boa, E. (2006) Basil little leaf: A new disease associated with a Phytoplasma of the 16SrI (aster Yellows) group in Cuba. *Plant Pathology*, **55**, 822.

Arocha, Y., Piñol, B., Acosta, K., Almeida, R., Devonshire, J., Van de Meene, A., Boa, E., Lucas, J. (2009) Detection of phytoplasma and potyvirus pathogens in papaya (*Carica papaya* L.) affected with 'Bunchy Top Symptom' (BTS) in eastern Cuba. *Crop Protection*, **28**, 640-646.

Baranwal, V.K., Un Nabi, S., Yadav, M.K. (2021) Plant virus diagnostics: traditional to recent and emerging advances. *Emerging Trends in Plant Pathology*. Springer Singapore, pp. 97–111.

Bertaccini, A., Fiore, N., Zamorano, A., Tiwari, A.K., Rao, G.P. (2019a) Molecular and serological approaches in detection of phytoplasmas in plants and insects. Phytoplasmas: Plant Pathogenic Bacteria - III. *Phytoplasmas: Plant Pathogenic Bacteria - III*. Springer Singapore, pp. 105-136.

Bertaccini, A., Paltrinieri, S., Contaldo, N. (2019b) Standard detection protocol: PCR and RFLP

analyses based on 16S rRNA gene. *Methods in Molecular Biology*, **1875**, 83-95.

Bruni, R., Bellardi, M.G., Parrella, G. (2016) Change in chemical composition of sweet basil (*Ocimum basilicum* L.) essential oil caused by alfalfa mosaic virus. *Journal of Phytopathology*, **164**, 202-206.

Carr, J.P. (2018) Tobacco mosaic virus. *Annual Plant Reviews online*. John Wiley & Sons, Ltd, Chichester, UK, 11, 27-67.

Chapman, S.N. (1998) Tobamovirus isolation and RNA extraction. *Methods in Molecular Biology (Clifton, N.J.)*, **81**, 123-129.

Clark, M.F., Adams, A.N. (1977) Characteristics of the microplate method of enzyme linked immunosorbent assay for the detection of plant viruses. *Journal of General Virology*, **34**, 475-483.

Davino, S., Accotto, G.P., Masenga, V., Torta, L., Davino, M. (2009) Basil (*Ocimum basilicum*), a new host of Pepino mosaic virus. *Plant Pathology*, **58**, 407-407.

Edwardson, J.R., Christie, R.G. (1978) Use of virus-induced inclusions in classification and diagnosis. *Annual Review of Phytopathology*, **16**, 31-55.

Edwardson, J.R., Christie, R.G. (1986) Tobacco mosaic virus cytopathological effects. *The Plant Viruses*. Springer US, Boston, MA, pp. 153-166.

El-Attar, A.K., Mokbel, S.A., El-Banna, O.H.M. (2019) Molecular characterization of alfalfa mosaic virus and its effect on basil (*Ocimum basilicum*) tissues in Egypt. *Journal of Virological Sciences*, **5**, 97-113.

El-Saad, A.A., El-Saad, A.K.A. (2018) Some ecological aspects of main pests and predators incidence on sweet basil in Assiut governorate, Egypt. *Journal of Phytopathology and Pest Management*, **5**, 29-42.

Ermacora, P., Osler, R. (2019) Symptoms of phytoplasma diseases. *Methods in Molecular Biology*. Humana Press Inc., **1875**, 53-67.

Esau, K. (1967) Anatomy of plant virus infections. *Annual Review of Phytopathology*, **5**, 45-74.

Fraser, R.S.S., Loughlin, S.A.R. (1982) Effects of temperature on the Tm-1 gene for resistance to tobacco mosaic virus in tomato. *Physiological Plant Pathology*, **20**, 109-117.

Grausgruber-Gröger, S. (2012) First report on natural occurrence of tomato spotted wilt Tospovirus in basil (*Ocimum basilicum*). *New Disease Reports*, **26**, 12-12.

Heinlein, M. (2002) The spread of Tobacco mosaic virus infection: Insights into the cellular mechanism of RNA transport. *Cellular and Molecular Life Sciences (CMLS)*, **59**, 58-82.

Holcomb, G.E., Valverde, R.A., Sim, J., Nuss, J. (1999) First report on natural occurrence of tomato spotted wilt Tospovirus in basil (*Ocimum basilicum* L.). *Plant Disease*, **83**, 966-966.

Honjo, M.N., Emura, N., Kawagoe, T., Sugisaka, J., Kamitani, M., Nagano, A.J., Kudoh, H. (2020) Seasonality of interactions between a plant virus and its host during persistent infection in a natural environment. *ISME Journal*, **14**, 506-518.

Hull, R. (2009) Mechanical inoculation of plant viruses. *Current Protocols in Microbiology*, **13**, 16B-6.

Jung, H.W., Yun, W.S., Hahm, Y.I., Kim, K.H. (2002) Characterization of tobacco mosaic virus isolated from potato showing yellow leaf mosaic and stunting symptoms in Korea. *Plant Disease*, **86**, 112-117.

Lebsky, V., Hernández-González, J., Arguello-Astorga, G., Cardenas-Conejo, Y., Poghosyan, A. (2011) Detection of phytoplasmas in mixed infection with begomoviruses: A case study of tomato and pepper in Mexico. *Bulletin of Insectology*, **64**, 2-4.

Lee, I. Ming, Davis, R.E., Dawn, E. (2000) Phytoplasma: Phytopathogenic Mollicutes. *Annual Review of Microbiology*, **54**, 221-225.

Li, D., Chen, P., Shi, A., Shakiba, E., Gergerich, R., Chen, Y. (2009) Temperature affects expression of symptoms induced by soybean mosaic virus in homozygous and heterozygous plants. *Journal of Heredity*, **100**, 348-354.

Marcone, C. (2009) Movement of phytoplasmas and the development of disease in the plant. In: "*Phytoplasmas: Genomes, Plant Hosts and Vectors*," pp. 114-131. CABI Publishing.

Martelli, G.P., Russo, M. (1977) Plant virus inclusion bodies. *Advances in Virus Research*, **21**, 175-266.

Musetti, R. (2013) Dienes' staining and light microscopy for phytoplasma visualization. In: *"Phytoplasma",* pp. 109-113. Humana Press, Totowa, NJ.

Nassar, M.A.E.A., El-Segai, M. U., Azoz, S.N. (2014) Anatomical and phytochemical studies on *Ocimum basilicum* L. nassar. Plant (Lamiaceae). *International Journal of Advanced Research*, **2**, 204-226.

Ong, S., Jonson, G.B., Calassanzio, M., Rin, S., Chou, C., Oi, T., Sato, I., Takemoto, D., Tanaka, T., Choi, I. R., Nign, C., Chiba, S. (2021) Geographic distribution, genetic variability and biological properties of rice orange leaf phytoplasma in Southeast Asia. *Pathogens*, **10**, 1-14.

Otulak, K., Chouda, M., Bujarski, J., Garbaczewska, G. (2015) The evidence of Tobacco rattle virus impact on host plant organelles ultrastructure. *Micron*, **70**, 7-20.

Parrella, G., Nappo, A.G., Delecolle, B. (2015) Cytopathology, biology and molecular characterization of two Italian isolates of Malva vein clearing virus. *Plant Science Today*, **2**, 69-73.

Purushothaman, B., Srinivasan, R.P., Suganthi, P., Ranganathan, B., Gimbun, J., Shanmugam, K. (2018) A comprehensive review on *Ocimum basilicum*. *Journal of Natural Remedies*, **18**, 71-85.

Rubab, S., Bahadur, S., Hanif, U., Iqbal, A., Sadiqa, A. (2020) Phytochemical and antimicrobial investigation of methanolic extract/ fraction of *Ocimum basilicum* L.". *Biocatalysis and Agricultural Biotechnology*, **31**, 101894.

Sanz, N. T., TsangHai, C., PoYung, L., (2001) A newly discovered mosaic disease of bush basil *(Ocimum basilicum*) in Taiwan. *Plant Pathology Bulletin*, **10**, 155–164.

Sastry, K. S., Mandal, B., Hammond, J., Scott, S. W., Briddon, R. W., (2019) *Encyclopedia of Plant Viruses and Viroids*. Springer India.

Schneider, H., (1973) Cytological and histological aberrations in woody plants following infection with viruses, Mycoplasmas, Rickettsias, and Flagellates. *Annual Review of Phytopathology*., **11**, 119–146.

Stevens, W.A. (1983) Symptoms of plant virus infection. In: "*Virology of Flowering Plants*," pp. 16–40. Springer US, Boston, MA, .

Wintermantel, W.M., Natwick, E.T. (2012) First report of alfalfa mosaic virus infecting basil (*Ocimum basilicum*) in California. *Plant Disease*, **96**, 295–295.

Wu, J.H., Rappaport, I. (1961) An analysis of the interference between two strains of tobacco mosaic virus on *Phaseolus vulgaris* L. *Virology*, **14**, 259–263.

Zahn, V., Dahle, J., Pastrik, K.H. (2011) Validation of ELISA for the detection of potato virus antigen in sap of potato plant leaves. *EPPO Bulletin*, **41**, 30–38.

التغيرات الباثولوجية لنبات الريحان المصاب بعدوى مختلطة من فيروس تبرقش الدخان والفيتوبلازما

ياسمين أبوهديمة، السيد طارق عبد السلام، محاسن إسماعيل، مها الخازندار
قسم النبات والأحياء الدقيقة - كلية العلوم - جامعة القاهرة - الجيزة - مصر.

تم فحص نبات الريحان (نبات طبي) والذي ظهرت عليه أعراض مرضية تتضمن التبرقش، وتشوه الأوراق، والتجاعيد، والتفرع الغزير للبراعم الإبطية (مكنسة السحرة) والتورق. وقد تبين أن النباتات مصابة بفيروس تبرقش الدخان والفيتوبلازما. تمت الإشارة إلى فيروس تبرقش الدخان نتيجة لإيجابية اختبار DAS-ELISA. وتم التعرف على الإصابة بالفيتوبلازما عن طريق تحاليل البيولوجيا الجزيئية باستخدام بادئات الفيتو بلازما P1/ P7 و البادئات المتداخلة R16F2n / R16R2 و التي نتج عنها قطع من الحمض النووي بطول 1200 قاعدة مزدوجة. هذا وقد تم نقل الفيروس ميكانيكيا بنجاح إلى نبات الدخان والداتورا بنوعيها ميتيل واستارمونيوم أيضا إلى الفاصولياء. أظهر الفحص المجهري للضوء وجود الأجسام متعددة الأشكال الخاصة بالفيتوبلازما بينما أوضح المجهر الإلكتروني النافذ وجود أجسام عصوية الشكل يبلغ طولها حولي 300 نانونتر والخاصة بفيروس تبرقش الدخان.

أسفرت الدراسات الهيستوباثولوجية والسيتوباثولوجية عن تغيرات في السلوك الخلوي لأوراق الريحان المصابة بفيروس تبرقش الدخان والفيتوبلازما. حيث لوحظ ضمور نسيجي وفرط تنسج في مناطق التبرقش في النسيج الوسطي للورقة. وقد لوحظ أيضا تغيرات في الأنسجة الوعائية وتنكس العضيات في القطاعات الرقيقة من النسيج الوسطي المصاب. هذا وقد كان وجود خلايا الفيتوبلازما والأجسام البلورية مؤشرا على الإصابة المختلطة. هذا هو التقرير الأول لعدوى مختلطة من فيروس تبرقش الدخان و الفيتوبلازما على نبات الريحان.